# NUMERICAL ANALYSES OF DIFFERENT STATE OF FLIGHT OF NEW CONCEPT COAXIAL ROTOR DEDICATED TO UNMANNED HELICOPTERS

Łukasz Czajkowski, lukasz.czajkowski@ilot.edu.pl, Łukasiewicz Research Network Institute of Aviation (Poland)

Małgorzata Wojtas, malgorzata.wojtas@ilot.edu.pl, Łukasiewicz Research Network Institute of Aviation (Poland)

Jarosław Stanisławski, jaroslaw.stanislawski@ilot.edu.pl, Łukasiewicz Research Network Institute of Aviation (Poland)

Kazimierz Szumański, kazimierz.szumanski@ilot.edu.pl, Łukasiewicz Research Network Institute of Aviation (Poland)

**Abstract**

Paper presents a concept analysis of a resilient coaxial main rotor designed in the Warsaw Institute of Aviation which incorporates features of a standard joint rotor with a rigid Active Blade Concept (ABC) rotor. The combination of two extreme cases aims to increase the cruising speed compared to classical joint rotors and cost reduction compared to technologically advanced ABC rotor. In the paper detailed numerical analysis of the rotor has been carried out based on the data obtained during bench and field tests carried out on the rotor blades and the rotor assembly. The calculations were conducted for envelope of deferent flight state: hover, horizontal flight level with different speeds, pull-up maneuver and analysis of high-speed flight (over 300 km/h). Results of calculations among others prove that a properly selected stiffness of the rotor blade attached to a rigid rotor hub allows for reduction of the separation distance between rotors compared to coaxial rotors with articulated blades.

## NOMENCLATURE

| | | |
|---|---|---|
| $I_{xi}$, $I_{yi,}$ $I_{zi}$ | - | Inertia moment |
| $m_i$ | kg | Lumped mas |
| $l_i$ | m | Blade segment |
| $T_z$ | N | Thrust |
| H | N | Longitudinal force, perpendicular to the shaft axis (azimuth180$^o$) |
| S | N | Lateral force, perpendicular to the shaft axis, (azimuth 90$^o$) |
| $M_x$ | Nm | Rolling moment (azimuth 270$^o$) |
| $M_y$ | Nm | Pitching moment (diving) |
| N | kW | Power |
| $R_n$ | - | Normal rotor |
| $R_s$ | - | Stiff rotor |

## 1. INTRODUCTION

The area of Unmanned Aerial Vehicles (UAVs) has seen rapidly growth over the last years. The one of the main reason for the increase in the use and development of unmanned aircraft is their ability to effectively carry out a wide range of applications with low cost and without putting human resources at risk [1].

New UAV solutions are being sought for both civilian and military users. The requirements for unmanned aircraft today are being dictated not only by the army but also by private sector. There are several directions in which unmanned flying platform are being developed. One of those direction is enhancing the safety of unmanned aerial vehicles, on the one hand, from the point of view of flight management systems for such platforms, on the other, the development of civil Aviation Regulations for UAV. Another is the use of new high-performance data transmission technologies and new sensors technique to increase unmanned aerial vehicles usability. At the same time, the emphasis is placed on the development possibilities of flying platforms in terms of tactical and technical parameters like: speed, ceiling, flight duration, but also in terms of maneuverability, resistance to extreme weather conditions and load capacity.

Now a days, development of UAVs of horizontal take-off and landing is observed. These are multi-impeller systems, classic helicopter systems with one main rotor and tail rotor, and less common systems with two coil rotors [1].

Before the start of any helicopter design process of a new solution, it is necessary to comprehensively analyze the character of work, the designed unit will be subject to. Parameters such as maximum take-off weight, maximum payload, operating range, maximum flight speed, economy of maintenance and operation, market trends, manufacturing technology, or the type of power supply should be taken into consideration.

Conventional helicopter rotor configuration are widely used because of their simplicity of implementation. The main advantages of such a design are simple design, light rotor hub, simple main transmission, low cost of manufacturing, and a vast knowledge based on existing solutions. Such systems, however, have experience some drawbacks. The major problem is anti-torque system which is required to counteract the one generated by the main rotor. For that purpose, most of the helicopters are equipped with an auxiliary rotor which can consume from 13% to even 30% of the total power at hover, depending on the helicopter construction. The literature [3, 4],



Presented at 45th European Rotorcraft Forum, Warsaw, Poland, 17-20 September, 2019

describes a further problem which appears during helicopter forward flight, this phenomenon is known as dissymmetry of lift in rotorcraft aerodynamics and refers to an uneven amount of lift on opposite sides of the rotor disc. Another issue occurs during helicopter landing. Greater precision of landing is required due to the risk of tilting the tail propeller to the ground.

Whereas [2] the coaxial rotor systems has relatively low face drag due to the short, properly shaped hull, small external dimensions, no tail rotor, increased load factor from 1 kilowatt of power, reduced diameter of the rotor, a small asymmetry of the lift force in the forward motion, simpler control due to mitigated aerodynamic forces, more stable flight, better stability in hover due to contrary side reactions of rotors in case of wind gusts. However they also have disadvantages, which include a complicated control devices and complicated power transmission, harmful interaction of both rotors, insufficient directional stability, danger of collision of the blades of both rotors.

Taking into considerations advantages and disadvantages of the above mentioned rotor configurations, a coaxial system was chosen to be implemented in an unmanned VTOL unit that does not exceed 450 kg of a takeoff weight. The coaxial system was chosen because it is a compact solution, resistant to problematic issues that occur in hulls that incorporate a tail rotor.

This paper presents a concept analysis of a resilient coaxial main rotor designed in the Warsaw Institute of Aviation which incorporates features of a standard joint rotor with a rigid Active Blade Concept (ABC) rotor. The combination of two extreme cases aims to increase the cruising speed compared to classical joint rotors and cost reduction compared to technologically advanced ABC rotor [6, 7].

In the paper detailed numerical analysis of the rotor has been carried out based on the data obtained during bench and field tests carried out on the rotor blades and the rotor assembly. The calculations were conducted for envelope of deferent flight state:

- hover;
- horizontal flight level;
- pull-up;
- high-speed flight (over 300 km/h).

## 2. COAXIAL ROTOR ANALYSIS

### 2.1. Main Rotor Model

Main Rotor model consists of rotor hub with rotor blade connectors and blades. In the computational algorithm, a multi-blades analysis was carried out. For a given moment of time, different parameters of motion and loads of individual blades located on different azimuths of the rotor disk were determined.

The real structure of blades and hub arms are replaced by the elastic axes with sets of lumped masses distributed along the radius of blades (as shown in Figure 1). The blades are divided into segments, which are substituted by lumped masses represent the inertial features of the blades. The elastic axes are divided into sectors, located between cross-sections of the neighboring lumped masses. The blade bending and torsion stiffness are assigned to section of the elastic axes. The following assumptions are applied to define the physical model of rotor:

- inertial, stiffness and geometrical features of all rotor blades are the same;
- lumped masses represent the inertial features of the corresponding blade segments (mass mi, inertial moments $I_{xi}$, $I_{yi}$, $I_{zi}$);
- sectors of blade elastic axis connect the blade cross-sections including the lumped masses;
- blade elastic axis can be twisted and bent in the rotor revolution and thrust planes;
- the rotor blade are spring-mounted in relation to the three axes (horizontal, vertical and axial joints);
- the blade pitch axis takes coincident position to the non-deformed blade elastic axis.

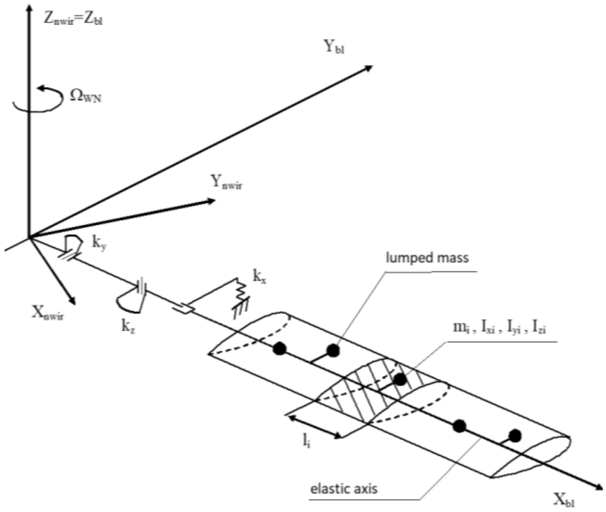


Fig. 1. Physical model of helicopter rotor includes blade elastic axes with sets of lumped masses [8]

The exact description of the mathematical model and algorithm used for calculations was discussed in literature [9, 10, 11].

### 2.2. Stand Tests

The calculation algorithm inter alia based on the real data input provides the forces and tensions that affect the rotor during different flight states. Most of input data was collected during rotor performance test on field bench and the blades stiffness tests [2]. Dynamic field test



Presented at 45th European Rotorcraft Forum, Warsaw, Poland, 17-20 September, 2019

(Figure 2) allowed, among others, define simplified polar characteristic of the coaxial rotor. While during rotor blades stiffness measurement (Figure 3) the distribution of stiffness in the plane of rotor rotation and thrust, as well as, torsional stiffness was determined.

Fig. 2. Coaxial rotor on a test stand

Fig. 3. Coaxial rotor blade stiffness measurement

The data obtained during those tests and measurement were used to calculate the forces that are applied on the rotor during helicopter flight, to predict the deflection of the rotor blades or calculate power consumption.

### 2.3. Analysis Assumtion

Several assumptions and simplifications were adopted before the analysis were carried out.

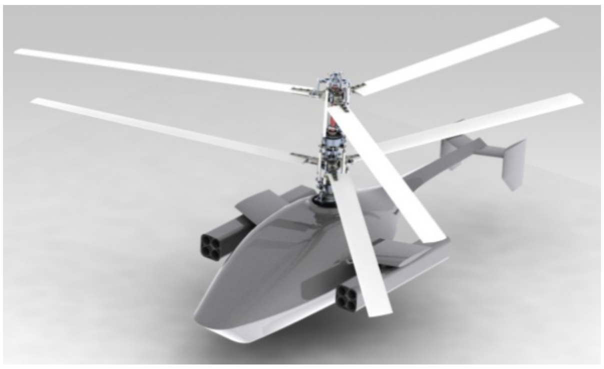

Fig. 4. Coaxial rotor implemented in a concept hull

One of the assumptions for the purpose of the calculations was to incorporated the rotor in a helicopter body (as shown in Figure 4) to take into account the drag forces acting on the hull during flight.

In the next step the blade and rotor head arm was divided into 23 sections as shown in figure 5.

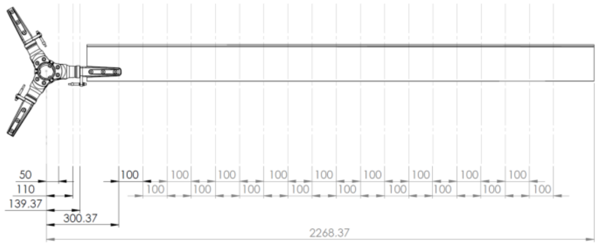


Fig. 5. Rotor hub arms and rotor blade cross-section

The division was made in such way that the determined sections of the calculation model corresponded to the measurement section of the stiffness distribution in real blade. Subsequently using the 3D model of rotor blade - rotor head unit and give material properties to the individual element we were able to determine the missing data, including masses and inertia moments of individual segments of hole assembly.

## 3. CALCULATION RESULTS

Using all obtained data including aerodynamic characteristics, deferent helicopter flight states were analyzed. The calculations also consider the possibility of increasing the rotor blades stiffness.

The coaxial configuration consisted of two three –bladed rotors. One of the important feature of the coaxial configuration is a vertical separation of upper and lower rotors, which should prevent collision of blades of counter-rotating rotors. In our case the distance between the lower and upper rotor is 0.5 meter.

The case of helicopter hover the upper rotor was treated as isolated one but for lower rotor inflow was increased by induced velocity coming from upper rotor. In hover with fulfilled condition of directional balance with equal power of both rotors, the upper rotor generated greater thrust than lower rotor (Table 1).

Tab. 1. Thrust and power of two rotors system in hover

| | Collective pitch, $^o$ | $T_z$, N | N, kW |
|---|---|---|---|
| Upper rotor | 16.326 | 2787.905 | 27.65 |
| Lower rotor | 17.110 | 1622.940 | 27.67 |
| Sum for upper and lower rotors | - | 4410.845 | 55.32 |



Presented at 45th European Rotorcraft Forum, Warsaw, Poland, 17-20 September, 2019

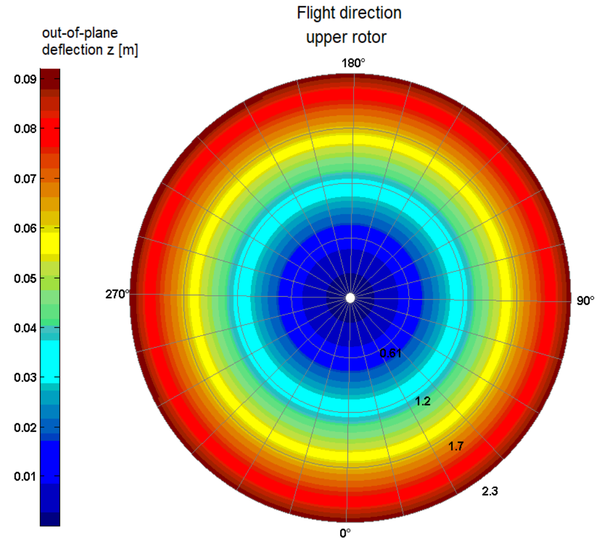


Fig. 6. Distribution of out-of-plane blade deflection at rotor disks in hover with for upper rotor

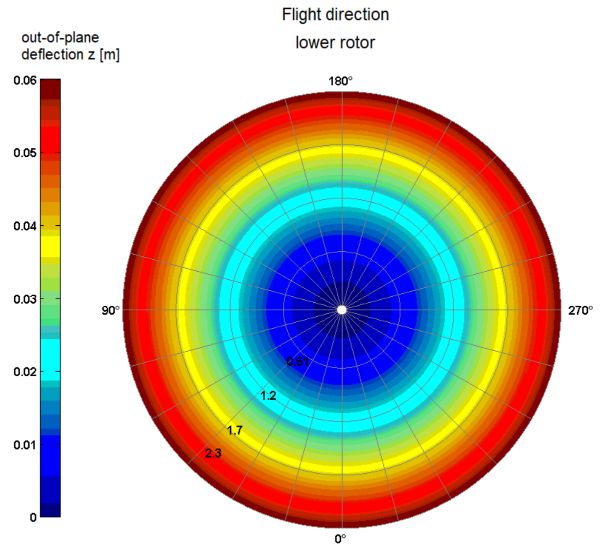


Fig. 7. Distribution of out-of-plane blade deflection at rotor disks in hover with for lower rotor

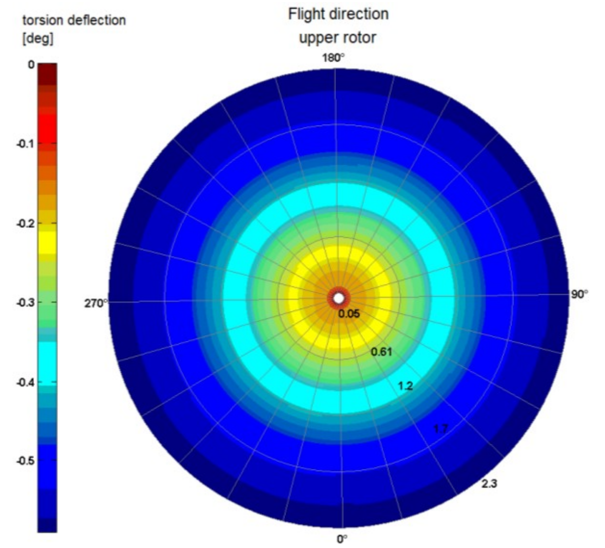


Fig. 8. Distribution of torsion blade deflection at rotor disks in hover with for upper rotor

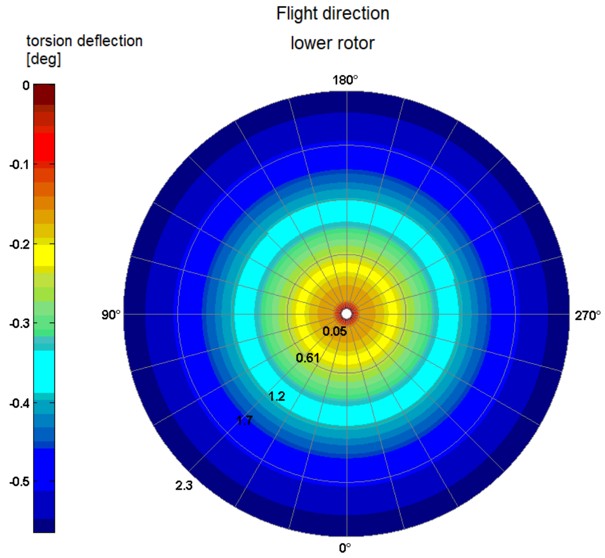


Fig. 9. Distribution of torsion blade deflection at rotor disks in hover with for lower rotor

Figure 6 to 9 shown out-of plane rotor blade deflection and torsion blade deflection for a upper and lower rotor in hover. The distribution of out-of-plane blade deflection for upper and lower rotor is small. Maximum deformation at the tip of the rotor blade is about 0.09 m for upper rotor, and 0.06 m for lower rotor.

Next discussed case concerns the pull-up maneuver when the helicopter is in hover. As in the previous case, the upper rotor was treated as isolated one with vertical speed about 2.5 m/s. While lower rotor inflow was increased by induced velocity coming from upper rotor and vertical speed of helicopter.

Table 2 shows the flight conditions of that case. At the pull-up maneuver when helicopter is in hover, the power consumption increases by about 18.5%.

Tab. 2. Thrust and power of two rotors system in hover with vertical velocity of 2.5 m/s

| | Collective pitch, ° | $T_z$, N | N, kW |
|---|---|---|---|
| Upper rotor | 17.670 | 2718.379 | 33.96 |
| Lower rotor | 18.850 | 1727.640 | 33.92 |
| Sum for upper and lower rotors | - | 4446,019 | 67,88 |

Figure 10 and 11 shown out - of plane rotor blade deflection for a upper and lower rotor with vertical speed about 2.5 m/s. As can be seen the flexural deformation of the rotor blades have not changed significantly.

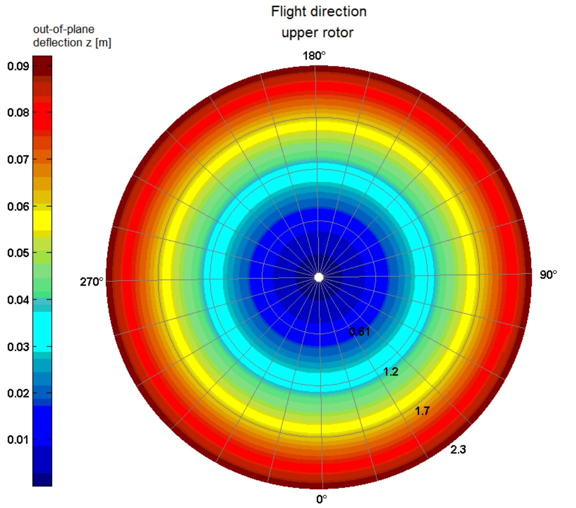


Fig. 10. Distribution of out-of-plane blade deflection at rotor disks in hover with vertical velocity of 2.5 m/s for lower rotor

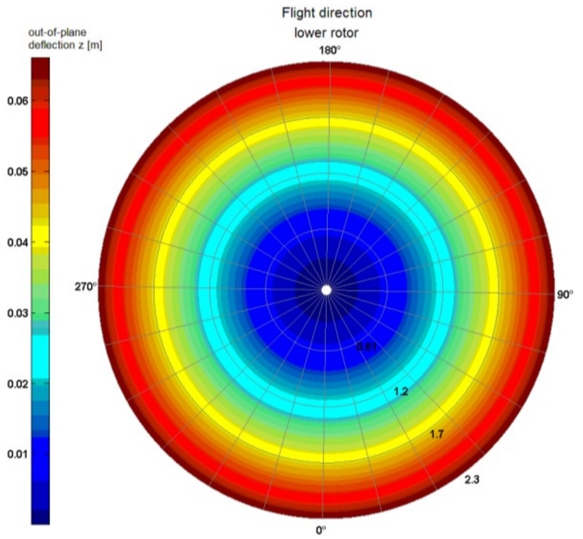


Fig. 11. Distribution of out-of-plane blade deflection at rotor disks in hover with vertical velocity of 2.5 m/s for lower rotor

In the cases of level flight due to large inflow through rotor disks coming from component of flight speed calculation of blade deflections were performed for rotors treated as isolated.

The following charts (Figure 12 – 14) shown distribution of blade parameters for disk of upper rotor in level flight at speed of V=100 km/h.

Char on Figure 12 show distribution of out-of-plane -z blade deflection. Maximum deflection according to azimuth $0^{o}$ is about 0,15 m.

In Figure 13 and 14 are shown distributions of blade torsion deflection and angle of attack at cross-sections of blade of the upper rotor. It can be noticed that the angles of blade torsion deflection comprise in the range between $-1.9^{o}$ and $1.3^{o}$.

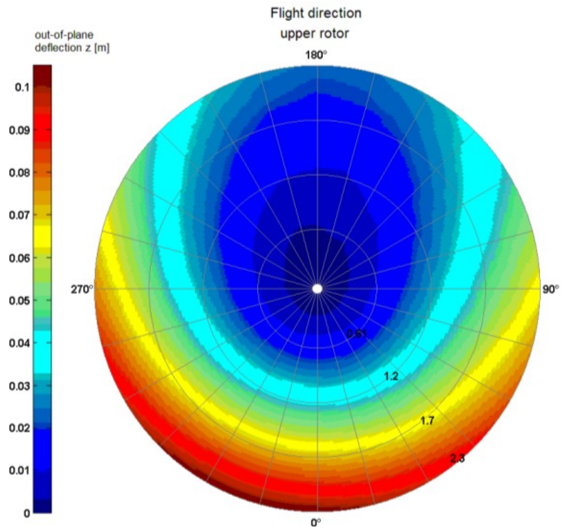


Fig. 12. Distribution of out-of-plane blade deflection at disk of upper rotor, in level flight at speed of V=100 km/h

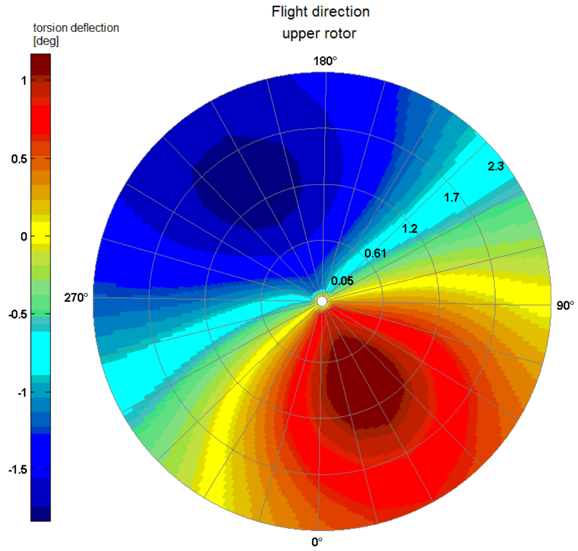


Fig. 13. Distribution of torsion blade deflection at disk of upper rotor, in level flight at speed of V=100 km/h

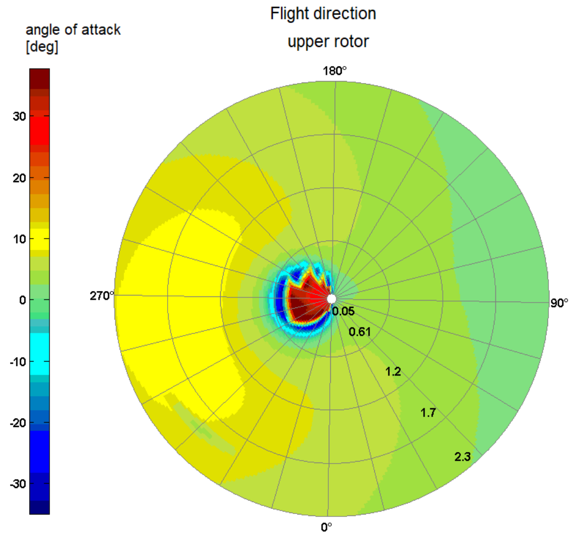


Fig. 14. Distribution of local angle of attack for disk of upper rotor in level flight at speed of V=100 km/h



Presented at 45th European Rotorcraft Forum, Warsaw, Poland, 17-20 September, 2019

In addition the analyzes out for several cruising speeds and for a rotor with a higher stiffness were carried. Blades stiffness parameters are increased as much as technology of production allows. Stiffness in the z - plane increased by 40%, stiffness in x –plane increased by 5% and torsional stiffness of blades increased by 50%.

Figures from 15 to 20 shown rotor thrust and power consumption, as well loads and moments occurring on the rotor depending on the speed of helicopter flight, for normal rotor ($R_n$) and stiffened rotor ($R_s$). The presented calculations refer to the upper rotor treated as isolated.

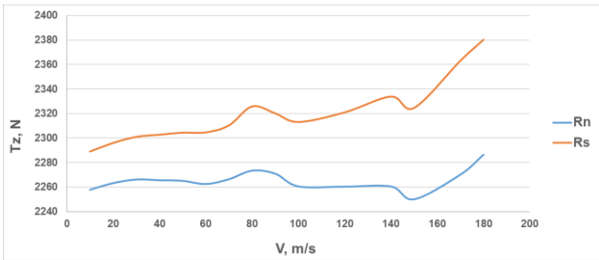


Fig. 15. Trust, for normal rotor ($R_n$) and stiffened rotor ($R_s$)

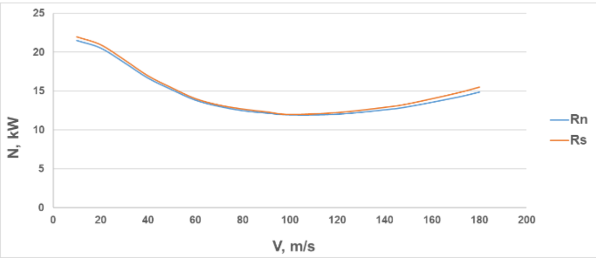


Fig. 16. Power consumption of normal rotor ($R_n$) and stiffened rotor ($R_s$)

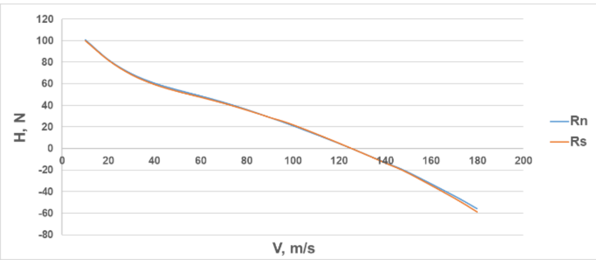


Fig. 17. Longitudinal force, perpendicular to the shaft axis, normal rotor ($R_n$) and stiffened rotor ($R_s$)

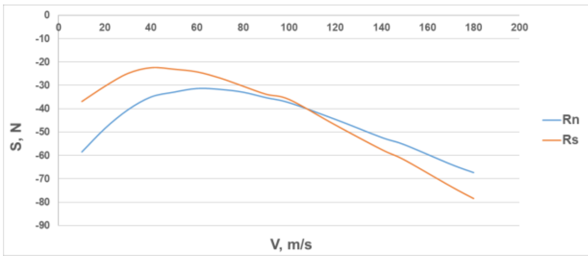


Fig. 18. Lateral force, perpendicular to the shaft axis, (azimuth 90$^o$), normal rotor ($R_n$) and stiffened rotor ($R_s$)

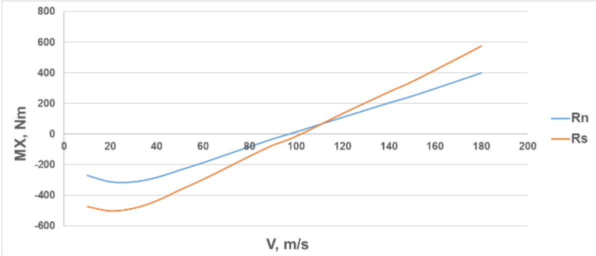


Fig. 19. Rolling moment (azimuth 270$^o$), for normal rotor ($R_n$) and stiffened rotor ($R_s$)

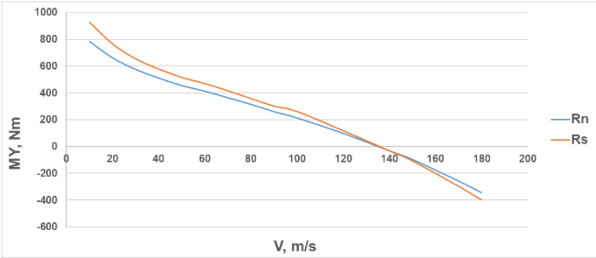


Fig. 20. Pitching moment (diving), for normal rotor ($R_n$) and stiffened rotor ($R_s$)

From analysis (Figure 18 and 19) it can be concluded that the use of a stiffer main rotor slightly changes the longitudinal force, perpendicular to the shaft axis (azimuth 180). However lateral force, perpendicular to the shaft axis, (azimuth 90$^o$) at flight level of speeds lower than 100 km/h is reduced. Using stiffer rotor, it can be achieve thrust increase of about 3%, with almost the same power consumed by the rotor (Figure 16 and 17).

The moments acting on the rotor shaft (Figure 19 and 20), in case the stiffer rotor, increase by approximately: 50% for rolling moment (at azimuth 270$^o$) and 12% for pitching moment.

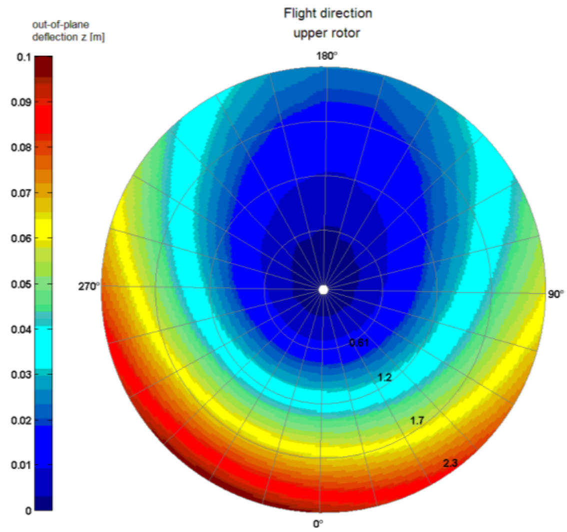


Fig. 21. Distribution of out-of-plane blade deflection at disk of upper rotor, in level flight at speed of V=100 km/h (for stifed rotor $R_s$)



Presented at 45th European Rotorcraft Forum, Warsaw, Poland, 17-20 September, 2019

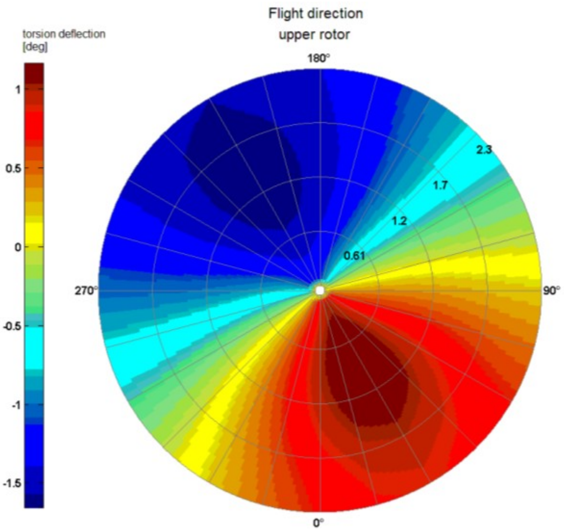


Fig. 22. Distribution of torsion blade deflection at disk of upper rotor, in level flight at speed of V=100 km/h (for stiffened rotor $R_s$)

In Figure 21 is shown distribution of out-of-plane -z blade deflection for upper stiffened rotor ($R_s$). Maximum deflection according to azimuth $0^o$ is about 0,10 m. While the Figure 22 is shown distributions of blade torsion deflection at cross-sections of blade of the upper stiffened rotor ($R_s$). It can be noticed that the angles of blade torsion deflection comprise in the range between $-1.7^o$ and $1.4^o$.

Considering the above analysis for each case, the best rotor parameters, are at flight level with speed of 100 km/h. Given that the rotor is dedicated to unmanned helicopters, it can be safely assumed that the flight speed can be up to about 180 km/h.

Tab. 3. Rotor parameters for flight level with speed of 316 km/h, for upper rotor

| Parameters | Unit | |
|---|---|---|
| Collective pitch, | o | 21.80 |
| $T_z$ | N | 2347.35 |
| N | kW | 37.84 |
| H | N | -245.67 |
| S | N | 224.72 |
| $M_x$ | Nm | 967.53 |
| $M_y$ | Nm | -1868.34 |
| Max and Min z - out of plane deflection (azimuth 180) | m | +19.68<br>- 18.81 |

However, when considering increasing the flight speed above 300 km/h, several problems occurring. The pitch of the rotor shaft (at azimuth 180), in a very fast flight, oscillates around $17.5^o$. Obtaining such an angle is difficult, among others for design reasons. In addition, to achieve the required lift force, the collective pitch of the rotor blades should be set around $21^o$ to $22^o$. This situation (data showed in Table 3) causes very large moments and forces acting on the rotor shaft. Also generate large rotor vibrations, and dangerous blade deflection in z - out of plane, which can lead to rotor destruction.

## 4. CONCLUSION

Conducted analyzes indicate that the proposed coaxial rotor solution has significant advantages over classic rotor solution. The rotor can reach thrust within 5 kN, which makes it unique on the ultra-light class drone market.

The most economical flight level speed, for both the Rn rotor and Rs rotor, is 100 km/h. This is related to the optimal power consumption and trust generation by the rotor as well as averages loads occurring on the rotor construction.

Change of rotor stiffness affects on blade deflection, mainly during horizontal flight. In the case of a stiffened rotor ($R_s$), the blade deformation is smaller. In addition, a slight increase of the rotor thrust is obtained, with practically the same power consumption. It is important, when selecting stiffness of the rotor, to pay attention to the rolling moment $M_x$ (azimuth $270^o$), which for the discussed the rotor increases by about 50%.

Analysis of simulation results prove that a properly selected stiffness of the rotor blade attached to a rigid rotor hub allows for reduction of the separation distance between rotors compared to coaxial rotors with articulated blades.

For very high speeds (over 300 km/h) it is necessary to ensure that the helicopter is equipped e.g. with a pushing propeller to minimize the inclination of the helicopter rotor shaft, thus significantly reducing the moments and forces occurring on the rotor.

## REFERENCES


[1] Alexisn K., Huerzeler Ch., Siegwart R., Hybrid predictive control of a coaxial aerial robot for physical interaction through contact, Control Engineering Practice, Vol. 32, pp. 96-112, 2014

[2] Czajkowski Ł., *Mechanical analysis process of a coaxial counter rotor for applications in unmanned ultra-light units*, Transactions on aerospace research, No. 2 (255) 2019, pp. 44–64

[3] Bramwell A.R.S, Done G., Balmford D., *Bramwell's Helicopters Dynamic*, 2nd edition, Butterworth-Heinemann, 2001

[4] Enconniere J., Ortiz-Carretero J., Pachidis V., *Mission performance analysis of a conceptual coaxial rotorcraft for air taxi applications,* Aerospace Science and




Presented at 45th European Rotorcraft Forum, Warsaw, Poland, 17-20 September, 2019

Technology, Vol. 69, pp. 1-14, 2017
[5] Ferguson, K. M., Thomson, D. G., Flight dynamics investigation of compound helicopter configurations, AHS 69th Annual Forum, Phonix, Arizona, May 22-23, 2013.
[6] Mainz H., Van der Wall B.G., *ABC rotor blades: design, manufacturing and testing*, paper 118 31th European Rotorcraft Forum, Florence, Italy, September 13-15, 2005
[7] Mokhtari R. M., Braham A. C., Cherki B., *Extended State Observer based control for coaxial-rotor UAV*, ISA Transactions, Vol. 61, pp. 1-14, 2016
[8] Stanisławski J., *Simulation investigation of operational conditions of rotor for high-speed compound helicopter*, Journal of KONES Powertrain and Transport, Vol. 25, No. 1, pp. 263 – 370, 2018
[9] Stanisławski J., *Performance requirements and simulation of rotor operation for high-mountain rescue helicopter*, Journal of KONES Powertrain and Transport, Vol. 25, No. 2, pp. 241 – 348, 2018
[10] Stanisławski J., *Experimental measurements and simulation calculations of loads in control system of helicopter rotor*, Transactions of the Institute of No.1, Vol. 238, pp. 35-53, 2015
[11] Stanisławski J., *Pattern of helicopter rotor loads and blade deformations in some states of flight envelope*, Transactions of the Institute of No. 1 Vol. 238, pp. 70-90, 2015





Presented at 45th European Rotorcraft Forum, Warsaw, Poland, 17-20 September, 2019